

Band-notched Ultra-Wideband Bandpass Filter Using Dual-Mode Resonator Loaded Slotline

Xuehui Guan*, Tao Xiong, Fangqi Yang, Pin Wen, and Haiwen Liu

Abstract—In this article, a novel band-notched ultra-wideband (UWB) bandpass filter based on hybrid microstrip/slotline structure is proposed. A quad-mode stubs-loaded slotline resonator is fed by two orthogonal microstrip lines and ultra-wideband bandpass characteristic is excited. A stub-loaded dual-mode microstrip resonator is externally loaded to the quad-mode slotline resonator, and a notched band with sharp roll-off characteristic is achieved. The circuit model for the dual-mode microstrip resonator loaded slotline is given and analyzed. The proposed filter is designed and fabricated. Simulated and measured return losses are -12 dB/ -18 dB and -18 dB/ -10 dB in lower and higher passband. The return loss in the notched band is greater than 15 dB.

1. INTRODUCTION

Tremendous interest has been aroused in the exploration of UWB bandpass filters (BPFs) since the Federal Communications Commission (FCC) released the unlicensed frequency range from 3.1 to 10.6 GHz for commercial communication application in 2002 [1]. Traditionally, UWB BPFs can be realized by using microstrip-fed microstrip multi-mode resonator (MMR) [2–4]. Desired strong coupling between feed lines and MMR is achieved by extremely narrow gap, leading to critical fabrication precision requirements. Then aperture-backed microstrip line technique is used to achieve the desired strong coupling with relatively easy fabrication gap [5, 6]. Recently, broadside-coupled structures have received great attention due to the merit associated with the electromagnetic coupling [7, 8]. Resonators and feed lines are assigned in different layers and strong couplings can be achieved easily by control their positions.

UWB communication system, which covers a wide frequency range, may interfere with the existing wireless systems such as wireless local area network (WLAN). Realization of band notched UWB BPF is a feasible solution to eliminate the problem of interference with other narrow band applications, as compared to the use of extra filter. In [9, 10] open loop resonators are etched in the transition structure of a UWB BPF to produce notched bands. In [11, 12], a narrow notched band is produced by introducing an external loaded stepped-impedance resonator. External loaded resonators can be allocated in different layers so as to acquire size reduction. In our previous work, two open loop microstrip resonators are loaded to the slotline and a narrow stopband is realized [13].

In this article, a novel UWB BPF with a sharp notched band is proposed. Stubs-loaded slotline MMR is fed by two microstrip lines and UWB bandpass characteristic is achieved. By loading a stub-loaded dual-mode microstrip resonator to the slotline MMR, a notched band is created in the UWB passband. Circuit model for the coupling structure is given and analyzed. Notched band can be controlled by changing the dual-mode microstrip resonator. Results show that the proposed filter exhibits a bandwidth from 3.1 to 10.6 GHz with return loss greater than 15 dB and the attenuation in the notched band from 5.1 to 5.3 GHz is greater than 15 dB.

Received 24 March 2014, Accepted 2 May 2014, Scheduled 7 May 2014

* Corresponding author: Xuehui Guan (xuehuiguan@gmail.com).

The authors are with the School of Information Engineering, East China Jiaotong University, Nanchang 330013, China.

2. CIRCUIT DESIGN

2.1. Slotline UWB Filter

Figure 1 shows the configurations of the proposed band-notched UWB BPF. A stub-loaded dual-mode microstrip resonator and two microstrip feed lines are located on the top layer. In the bottom layer, there is a stubs-loaded slotline MMR. The MMR and the feed lines are folded and orthogonal coupling is achieved.

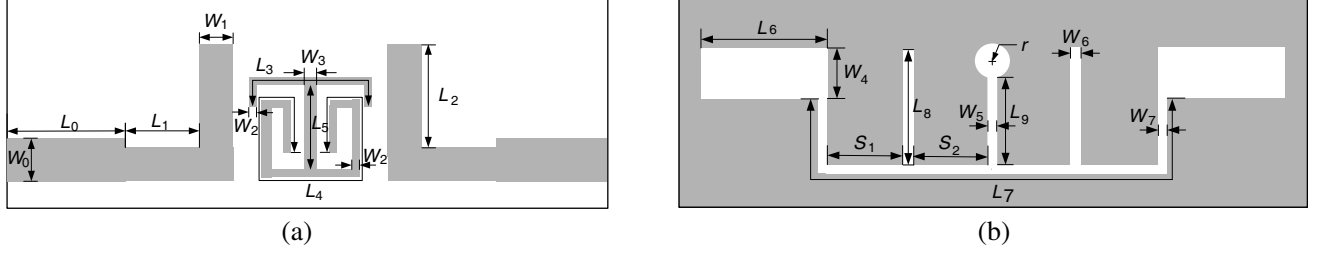


Figure 1. Configurations of the proposed filter. (a) Top view, (b) bottom view.

Slotline structure shows many advantages such as wide range of characteristic impedance, easy realization of high impedance than microstrip, and fully utilization of PCB board. The UWB bandpass characteristic is generated by the stubs-loaded slotline MMR, as shown in Fig. 1(b). Combining with the microstrip feed structure, desired strong coupling between feed line and the MMR can be easily achieved. The slotline MMR consists of a stepped impedance resonator and three loading stubs, with one locating at the middle of the resonator. Compared with traditional stepped-impedance resonator (SIR) and stub-loaded resonator (SLR), the proposed resonator has more degrees of freedom to control its resonant frequencies, which results in conveniently relocating the required resonant modes within the UWB band. Considering the influence of the folding of resonator and the impedance step, once the original parameters of the slotline resonator is determined, EM solver is invoked to tune the structure to achieve an optimized characteristic of the resonator. Fig. 2 depicts the simulated transmission characteristics of the resonator. The solid line and dashed line indicate the transmission characteristic of the resonator with and without the additional circle stub, respectively. Additional stub increases the electrical length of the whole central stub and another resonant mode is shown in the UWB range.

Because the proposed slotline MMR is a symmetrical structure evenodd theory can be applied to analysis its resonant characteristics. Fig. 3 shows equivalent circuits of the slotline MMR. In order to facilitate analysis, the radial stub has been replaced in terms of a rectangular stub. Under odd-mode

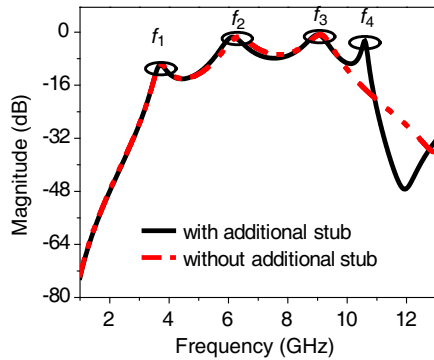


Figure 2. Characteristics of the MMR with and without the additional circle stub.

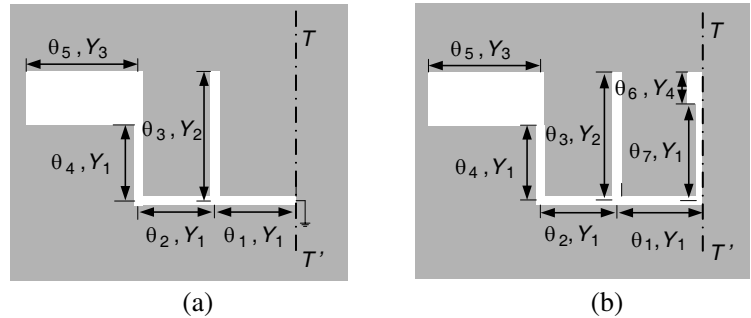


Figure 3. Equivalent circuits of slotline MMR. (a) Odd-mode, (b) even-mode.

excitation its resonant condition can be derived as,

$$Y_1^2 + Y_3 \tan \theta_4 \tan \theta_5 (Y_2 \tan \theta_1 \tan \theta_3 + \tan \theta_1 \tan \theta_2 - Y_1) + Y_2 \tan \theta_1 \tan \theta_3 - Y_1 \tan \theta_1 \tan \theta_2 \\ (Y_1 \tan \theta_2 \tan \theta_4 + Y_3 \tan \theta_4 \tan \theta_5 - Y_1) - Y_1 (Y_1 \tan \theta_4 + Y_3 \tan \theta_5) (\tan \theta_1 + \tan \theta_2) = 0 \quad (1)$$

Under even-mode excitation, its resonant condition can be summarized

$$(Y_1 - Y_3 \tan \theta_4 \tan \theta_5) [Y_1 Y_2 \tan \theta_3 (1 - \tan \theta_1 \tan \theta_7) + Y_1 Y_4 \tan \theta_6 (1 - \tan \theta_1 - \tan \theta_7 - \tan \theta_1 \tan \theta_7) \\ + Y_1^2 (\tan \theta_1 + \tan \theta_2 + \tan \theta_7 - \tan \theta_1 \tan \theta_2 \tan \theta_7) - Y_2 Y_4 \tan \theta_3 \tan \theta_6 (\tan \theta_1 + \tan \theta_7)] = 0 \quad (2)$$

It can be observed from Equation (1) that the odd mode resonances are exclusively dependent on the parameters of folded SIR and two sided-stubs, whereas the resonances frequencies of even excitations extracted in Equation (2) indicates that the even modes could be controlled by the loaded stub at the center section.

Next, influences of three parameters of the resonator on the resonant modes of the resonator are studied. Fig. 4 shows the variation of resonant-mode frequencies against L_6 , length of step impedance unit of stepped impedance resonator L_8 , length of the stub, and radius of the additional circle stub r . Four resonant modes (i.e., f_1 , f_2 , f_3 and f_4) are created in the studied frequency range, which are applied to generate the UWB bandpass transmission characteristic. Fig. 4(a) shows the variation of resonant modes against L_6 . As L_6 increases from 2.8 to 5.8 mm, f_1 drops from 4.1 GHz to 3.1 GHz, and f_2 drops from 6.5 GHz to 5.5 GHz, while f_3 and f_4 keep almost unchanged. Fig. 4(b) shows the variation of resonant modes against L_8 , the length of the sided stub. As L_8 increases from 2.8 to 4.8 mm, f_3 drops from 10.5 GHz to 8 GHz, and f_4 drops from 11.5 GHz to 10 GHz, while f_1 and f_2 keep almost

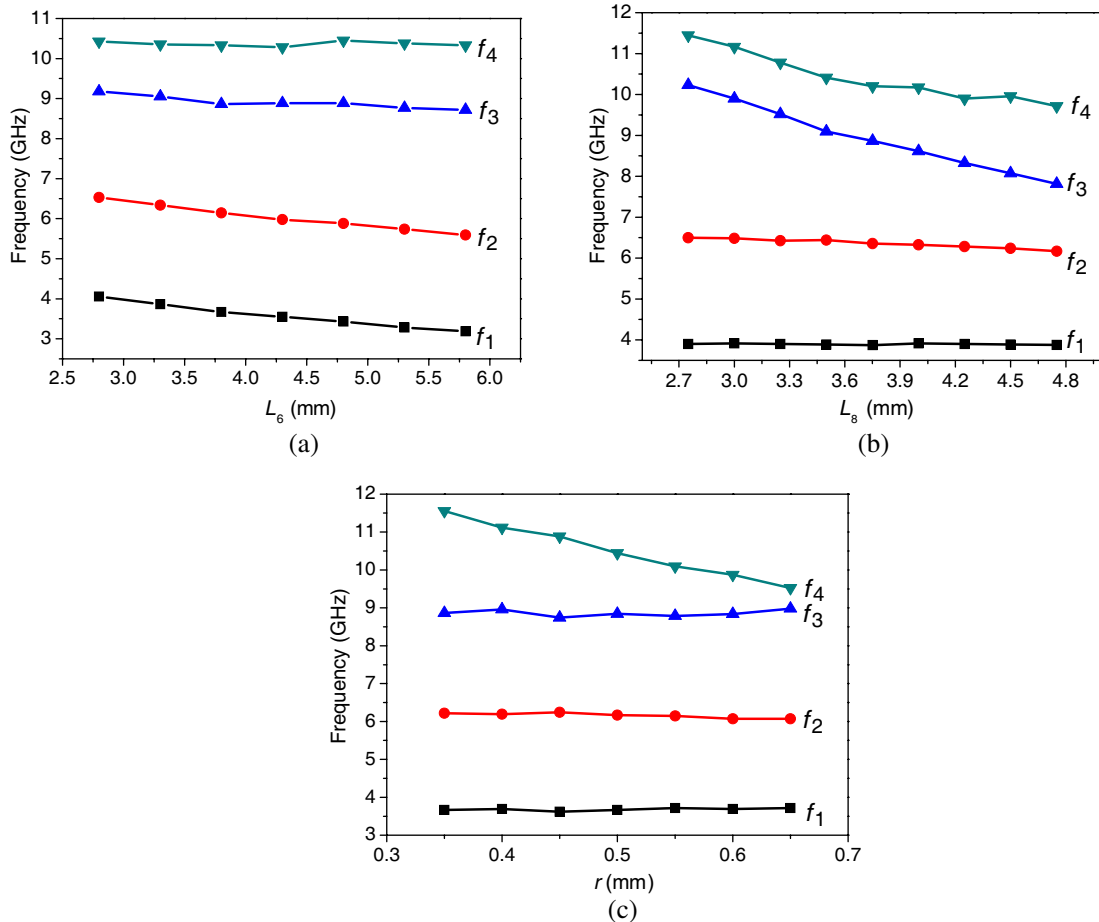


Figure 4. Resonant-mode frequencies against (a) L_6 , (b) L_8 , and (c) r .

unchanged. Fig. 4(c) depicts the variation of resonant modes against the radius of the additional circle stub. As the radius r increases from 0.35 to 0.65 mm, f_1 , f_2 , and f_3 remain stationary while f_4 drops from 11.56 GHz to 9.53 GHz. These resonant frequencies are basically related to the stepped impedance resonator, and some ones also can be separately controlled by the loaded stubs, which shows great convenient in relocating the required resonant modes.

2.2. Realization of Notched Band

Based on the UWB filter mentioned above, a notched band is produced and a band-notched UWB BPF is designed. As shown in Fig. 1, the MMR of the proposed UWB BPF is located on the ground plane. To make full use of the space of the filter, a dual-mode stub-loaded microstrip resonator on the top layer is loaded to the slotline resonator.

Figure 5(a) illustrates the circuit of a dual-mode resonator loaded slotline, where the white section indicates the slotline, the gray part is the ground, and the black one is a dual-mode microstrip resonator. Similar to the situation of loading a DGS to a microstrip line, it is a dual case and will form a stopband when the resonator works [14, 15]. Equivalent circuit of dual-mode resonator loaded slotline is provided in Fig. 5(b). Two resonant modes of the stub-loaded resonator are coupled to the slotline, providing a bypass for the adjacent signal of its resonance. The degree of separation of two modes determines the bandwidth of the notched band, and the coupling between resonator and slotline influences the amplitude of the attenuation.

Figure 6(a) shows the transmission characteristics of the resonator versus L , the length of the loading stub. When L increases from 4.5 to 6.0 mm, the lower resonant mode keeps unchanged, and the higher mode decrease from 3.06 GHz to 2.84 GHz. As we all know, the bandwidth of the bandstop filter are mainly determined by the separation of two transmission zeroes, so it can be adjusted by the length of the stub L . A transmission pole is also created near the lower transmission zero, sharpening the transition band. Fig. 6(b) illustrates the effect of varying S on the modes of the dual-mode resonator.

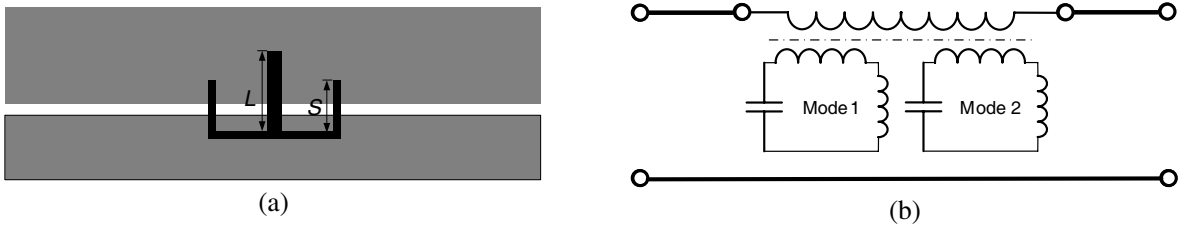


Figure 5. Dual-mode resonator loaded slotline. (a) Structure, and (b) its equivalent circuit model .

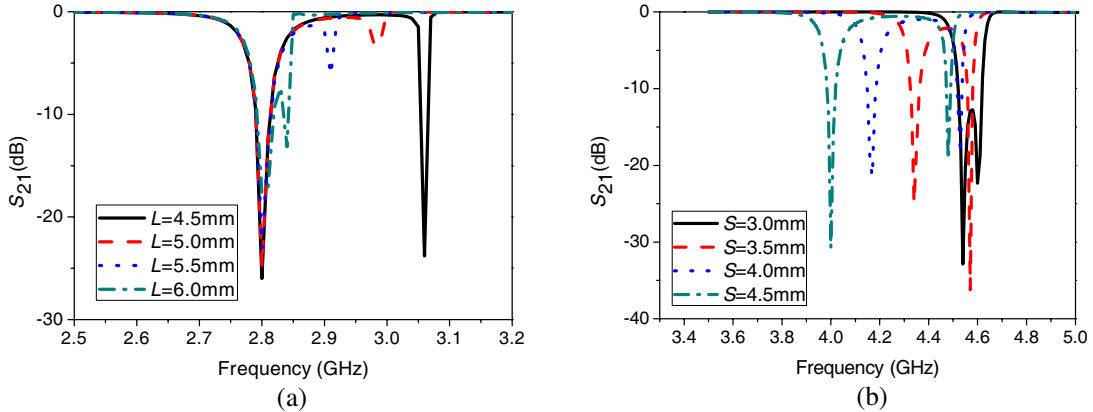


Figure 6. Transmission characteristics of simplified dual-mode resonator with varied parameters (a) L , and (b) S .

When S increases from 3.0 mm to 4.5 mm, the bandwidth of the filter increase from 60 MHz to 480 MHz and the central frequency decrease from 4.6 GHz to 4.2 GHz. Obviously, modifying S and L can change the position and the bandwidth of the stopband.

3. FILTER IMPLEMENTATION AND RESULTS

Based on the proposed structure, a UWB BPF with notched band from 5.15 GHz to 5.35 GHz is designed and fabricated. The feed lines and the MMR in slotline are folded and orthogonal coupled to acquire the desired strong coupling. A dual-mode stub-loaded open loop resonator is loaded to the slotline and a notched band for WLAN is produced. The dual-mode resonator is folded in order to improve the slow-wave effect for miniaturization. The filter is designed and fabricated on a 0.8 mm Taconic substrate with a relative dielectric constant of $\epsilon_r = 3.5$ and a dielectric loss tangent of 0.0018. Finally obtained parameters of the filter shown in Fig. 1 are: $L_0 = 4.8$ mm, $L_1 = 3.8$ mm, $L_2 = 4.7$ mm, $L_3 = 8.00$ mm, $L_4 = 17.40$ mm, $L_5 = 3.70$ mm, $L_6 = 3.80$ mm, $L_7 = 15.4$ mm, $L_8 = 3.5$ mm, $L_9 = 2.2$ mm, $W_0 = 1.8$ mm, $W_1 = 1.50$ mm, $W_2 = 0.30$ mm, $W_3 = 0.60$ mm, $W_4 = 1.50$ mm, $W_5 = 0.60$ mm, $W_6 = 0.30$ mm, $W_7 = 0.30$ mm, $S_1 = 2.45$ mm, $S_2 = 2.1$ mm, and $r = 0.55$ mm. Measurements are performed using vector network analyzer AV3926. A comparison between the simulated and measured results is shown in Fig. 7, where the solid lines and the dashed lines indicate the EM simulated results and measured results, respectively. Simulated results show that the 3 dB bandwidth of the filter covers from 3.1 GHz to 5.15 GHz and from 5.35 GHz to 10.6 GHz. While the measured ones show that the 3 dB bandwidth covers from 3.2 GHz to 5.15 GHz and from 5.35 GHz to 10.6 GHz. Simulated and measured insertion losses of each passband are about 2 dB, return losses are -12 dB/ -18 dB and -18 dB/ -10 dB. Return loss in the notch band is greater than 15 dB. In addition, the group delay within the passband is between 0.26 ns~ 0.75 ns. Except for the deviation that may be caused by the fabrication, the simulated results agree well with the measured results. The photographs of the fabricated filter are shown in Fig. 8. The size of the circuit is about 28 mm \times 18 mm.

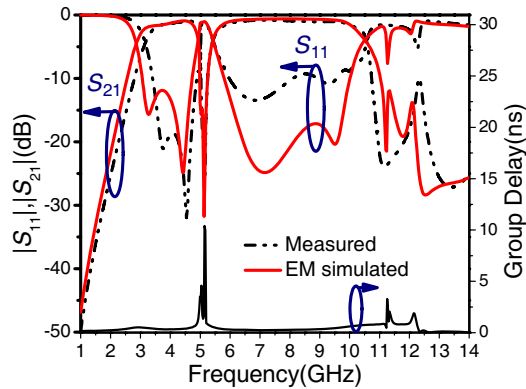


Figure 7. Comparison between measured and EM simulated results of the filter.

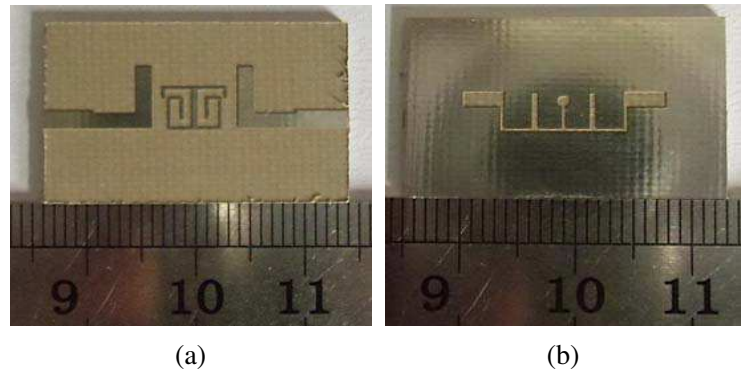


Figure 8. Photographs of the fabricated filter. (a) Top view, and (b) bottom view.

4. CONCLUSION

A band-notched UWB BPF using the hybrid slotline and microstrip is proposed. UWB characteristic is obtained by using the microstrip-fed stub-loaded slotline MMR. A notch band from 5.15 GHz to 5.35 GHz, which is designed for eliminating the WLAN signal, is realized by loading a stub-loaded dual-mode microstrip resonator to the slotline MMR. Good agreement between measured and simulated results demonstrates the proposed structure.

ACKNOWLEDGMENT

This work was supported by the National Natural Science Foundation of China (No. 61161005), Jiangxi Provincial Young Scientists Cultivation Program and 555 Talent Program of Jiangxi Province, all in China.

REFERENCES

1. Federal Communications Commission, "Revision of Part 15 of the commission's rules regarding ultra-wideband transmission systems," *First Report and Order*, FCC 02.V48, Apr. 2002.
2. Zhu, L., S. Sun, and W. Menzel, "Ultra-wideband (UWB) bandpass filters using multiple-mode resonator," *IEEE Microwave and Wireless Components Letters*, Vol. 15, 796–798, 2005.
3. Cai, P., Z. Ma, X. Guan, Y. Kobayashi, T. Anada, and G. Hagiwara, "Synthesis and realization of novel ultra-wideband bandpass filters using 3/4 wavelength parallel-coupled line resonators," *2006 Asia-Pacific Microwave Conference Proceedings*, 159–162, Dec. 2006.
4. Chen, H. and Y.-X. Zhang, "A novel and compact UWB bandpass filter using microstrip fork-form resonators," *Progress In Electromagnetics Research*, Vol. 77, 273–280, 2007.
5. An, J. and G. M. Wang, "UWB filter using defected ground structure of von koch fractal shape slot," *Progress In Electromagnetics Research Letters*, Vol. 6, 61–66, 2009.
6. Wang, H. and L. Zhu, "Aperture-backed microstrip line multiple-mode resonator for design of a novel UWB bandpass filter," *2005 Asia-Pacific Conference Proceedings*, Suzhou, China, Dec. 2005.
7. Li, R. and L. Zhu, "Compact UWB bandpass filter on hybrid microstrip/slotline structure with improved out-of-band performances," *International Conference on Microwave and Millimeter Wave Technology Proceedings*, Chengdu, China, May 2008.
8. Li, K., D. Kurita, and T. Matsui, "An ultra-wideband bandpass filter using broadside-coupled microstrip-coplanar waveguide structure," *IEEE MTT-S Int. Dig.*, 675–678, Jun. 2005.
9. Hsiao, P. Y. and R. M. Weng, "Compact open-loop UWB filter with notched band," *Progress In Electromagnetics Research Letters*, Vol. 7, 149–159, 2009.
10. Chen, L., F. Wei, X.-W. Shi, and C.-J. Gao, "An ultra-wideband bandpass filter with a notched-band and wide stopband using dumbbell stubs," *Progress In Electromagnetics Research Letters*, Vol. 17, 47–53, 2010.
11. Chen, C. P., Y. Takakura, H. Nihie, Z. Ma, and T. Anada, "Design of compact notched UWB filter using coupled external stepped-impedance resonator," *2009 APMC Proc.*, Singapore, Dec. 2009.
12. Zhao, J., J. Wang, and J.-L. Li, "Compact microstrip UWB bandpass filter with triple-notched bands," *Progress In Electromagnetics Research C*, Vol. 44, 13–26, 2013.
13. Guan, X., P. Chen, W. Fu, H. Liu, and G. Li, "A novel ultra-wide band bandpass filter with notched band using slotline and microstrip resonators," *Microwave and Optical Technology Letters*, Vol. 53, 2949–2951, 2011.
14. Huang, J.-Q., Q.-X. Chu, and C.-Y. Liu, "Compact UWB filter based on surface-coupled structure with dual notched bands," *Progress In Electromagnetics Research*, Vol. 106, 311–319, 2010.
15. Lin, C. J., C.-C. Chiu, S.-G. Hsu, and H. C. Liu, "A novel model extraction algorithm for reconstruction of coupled transmission lines in high-speed digital system," *Journal of Electromagnetic Waves and Applications*, Vol. 19, No. 12, 1595–1609, 2005.